Quasi-Lumped Suspended Stripline Filters and Diplexers

Wolfgang Menzel, *Fellow, IEEE,* and Atallah Balalem

***Abstract*—This paper demonstrates a general concept and different types of filters and a diplexer realized in suspended stripline using quasi-lumped elements. Very small low-pass, bandpass, and high-pass filters with typically low loss are designed, fabricated, and tested; even transmission zeroes can easily be included into the design by additional coupling structures. Finally, a low-pass and high-pass filter are combined to form a diplexer of very small size.**

***Index Terms*—Bandpass filters, diplexers, filters, high-pass filters, low-pass filters, lumped-element circuits, stripline filters.**

I. Introduction

THE SUSPENDED stripline (SSL) has proven to be an excellent transmission-line system to realize different types of filters [1]–[4]. Compared to a microstrip or coplanar line, its larger cross section results in lower current densities on the metallization and lower electric-field strength in the dielectric and, therefore, reduced losses. Typically, however, metal losses dominate in these types of planar lines. Furthermore, no radiation occurs due to the shielding (mount) of the SSL. As a much higher portion of the electromagnetic field extends in air, dispersion is low as well. The necessary mount for the SSL, on the other hand, requires an increased fabrication effort.

Most of the filters realized in this technique up to now are mainly based on transmission-line structures like stubs and quarter- and half-wavelength resonators. Without additional effort, filter elements can be realized on both sides of the substrate [2]–[6]; even multisubstrate arrangements have been proposed [7].

Due to the larger cross section with a considerable amount of electromagnetic field in air, the effective dielectric constant of the SSL is rather low, and transmission-line elements get quite large. Therefore, SSL filters typically are not as small as highly integrated microwave and millimeter-wave front-ends require today. First approaches toward smaller filters using quasi-lumped elements have been made for low-pass filters based on very short very low-impedance lines for the capacitances and very short high-impedance lines for the inductances [4], [5], leading, at the same time, to very broad stopband performance due to the semilumped nature of their elements.

In this paper, a general approach for the realization of SSL lumped-element filters is described, and these principles are applied to the design of different bandpass and high-pass filters and diplexers. In addition, these techniques allow the implementation of additional coupling elements to achieve quasi-elliptic responses.

In Section II, the principle setup of the SSL structure as used in this study is explained, and an overview about the involved filter elements is given. The general design procedure for such filters is explained in Section III. Following this, some typical examples are given for SSL low-pass, bandpass, and high-pass filters, followed by a diplexer consisting of a low- and high-pass filter.

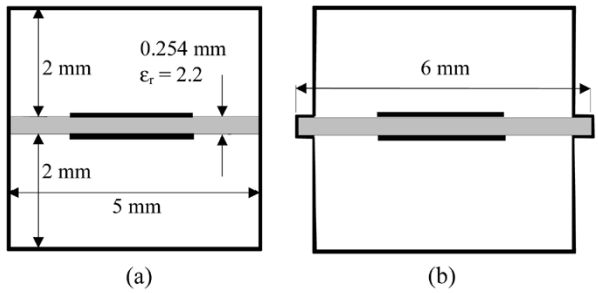

Fig. 1. (a) Ideal and (b) practical cross section of SSL as used in these investigations.

II. General Transmission Line and Filter Structures

A. SSL

The general structure of an SSL consists of a thin substrate suspended in the center of a metal channel (Fig. 1). The channel as used throughout this study is 5-mm wide, and 2 mm of air are provided above and below the substrate (RT Duroid, substrate thickness 0.254 mm, dielectric constant 2.22). For simulation purposes, the channel has a rectangular cross section [seeFig. 1(a)]; in the experimental setup, the channel has small groves at the sides to hold the substrate [see Fig. 1(b)]. With these small mount dimensions, filters can easily be realized in the 3–15-GHz frequency range. Due to the small cross section, effects of metal waveguide modes occur in this configuration above 20 GHz only. For filters at lower or higher frequencies, the structures as demonstrated here can be scaled in size.

As long as there is no metallization structure connected to the side of the mount, the dimensions are such that there is a negligible influence of the groves [8]. In case there is a shunt connection within a filter circuit, however, there is some influence on the circuit performance. The surface current on the metallization connected to the mount continues on the inner surface of the mount; on one side, the current has to flow around the grove, leading to some extra inductance.

Manuscript received March 20, 2005; revised May 25, 2005.

W. Menzel is with Microwave Techniques, University of Ulm, D-89069 Ulm, Germany (e-mail: wolfgang.menzel@ieee.org).

A. Balalem is with Microwave and Communication Engineering, University of Magdeburg, D-39016 Magdeburg, Germany.

Digital Object Identifier 10.1109/TMTT.2005.855139

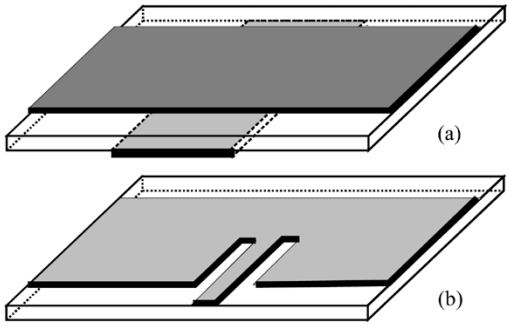

Fig. 2. Shunt SSL reactances. (a) Capacitance. (b) Inductance.

The general transmission-line properties of the ideal SSL are calculated using a spectral-domain method [9], the detailed filter structures finally are computed and optimized using a commercial simulator.[1]

All filters presented below have 50-Ω ports, resulting in SSL interconnect lines of 3.8-mm width. The filters as described in Sections IV–VI are placed in a mount of 30-mm length. Input and output lines are soldered to subminiature A (SMA) connectors. All experimental results are given with respect to the coaxial ports including the losses of transmission-line lengths between filter and ports and the transitions from the SSL to the coaxial measurement system. For comparison, a homogeneous SSL in this mount results in an insertion loss of approximately 0.1 dB at low frequencies and 0.3 dB at 20 GHz, respectively.

B. Filter Elements

Lumped-element filters require both series and shunt inductors and capacitors and their combination to form either series or parallel resonators. The SSL in the small mount as used here, together with the use of metal structures on both sides of the substrate, gives the ideal medium to realize all these elements. The following figures show a section of the SSL substrate with the basic layout of major SSL lumped elements. Connecting ports are on the left- and right-hand sides, respectively. Metal structures touching the front and back side edges are connected to the mount (ground).

A section of wide transmission line already provides capacitance versus ground; this can be increased by adding a ground metallization below the strip [see Fig. 2(a)]. A thin metal strip connected to the mount forms a shunt inductance; its inductive value can be increased and controlled by an inset in the main strip [see Fig. 2(b)].

A series inductance can easily be formed by a section of thin strip between wider connecting lines [see Fig. 3(a)]. Series capacitances can be realized in different ways—in the form of end coupling, overlapping of strips on the top and bottom layers of the substrate [see Fig. 3(b)], interdigital structures [see Fig. 3(c)], or by improving end coupling on one side of the substrate by an additional patch on the opposite side [see Fig. 3(d)].

As long as these structures are small compared to wavelength, their behavior calculated by full-wave methods can be approximated by equivalent lumped elements. This allows a first rough design of the required filter elements. For higher precision and at higher frequencies, however, their full-wave performance needs to be considered including electromagnetic coupling between the different elements.

[1]SONNET, ver. 9, Sonnet Software Inc., North Syracuse, NY.

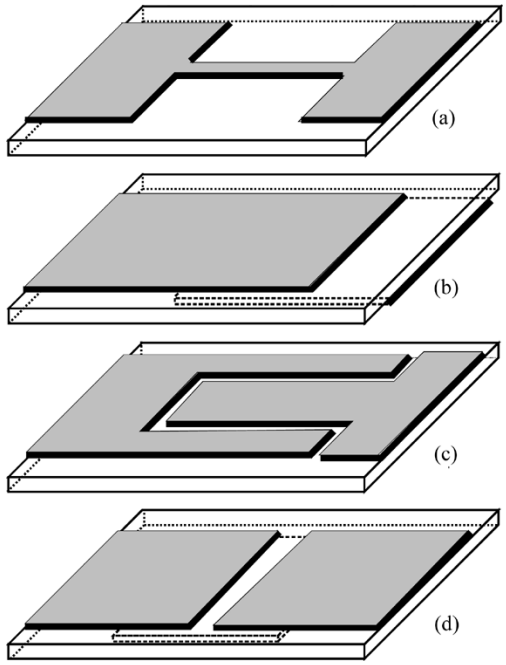

Fig. 3. Series reactances in SSL. (a) Inductance. (b) Capacitance formed by overlapping strips on opposite substrate sides. (c) Interdigital capacitance. (d) Capacitance formed by additional patch on backside of the substrate.

III. General Filter Design

The basic design procedure for all filters presented below is the same; its details are outlined in the following. Together with the description of the individual filters, specific design considerations are mentioned if necessary.

The filter elements, as described in Section II-B, form a filter building kit from which, at least in principle, different types of filters can be realized based on standard filter design. In addition, further elements can be added to improve the filter response, e.g., to achieve quasi-elliptic responses.

Filter design starts with a classical lumped-element equivalent circuit, e.g., according to [10]. These elements then have to be realized in the form of SSL structures, as depicted in Figs. 2 and 3. To this end, design charts are pre-calculated for different dimensions of the SSL elements or combinations of these using a full-wave simulator . As an example, Fig. 4 shows values of the series capacitance of single- and double-sided end coupling for 50-Ω lines (3.8-mm wide).

Another example is a shunt resonator, as can be used for bandpass filters [see Fig. 5(a)]. The patch type metallization forms a capacitance and the thin strip forms an inductance against ground. For the simulation of the element values, the ground connection of the narrow strip is opened, and the imaginary part of the input impedance into the structure is calculated. Comparing resonance frequency (the imaginary part is zero) and the derivative of the imaginary part with respect to frequency to the corresponding values of the equivalent circuit [see Fig. 5(b)], its elements can be determined [11]. The inductance formed by

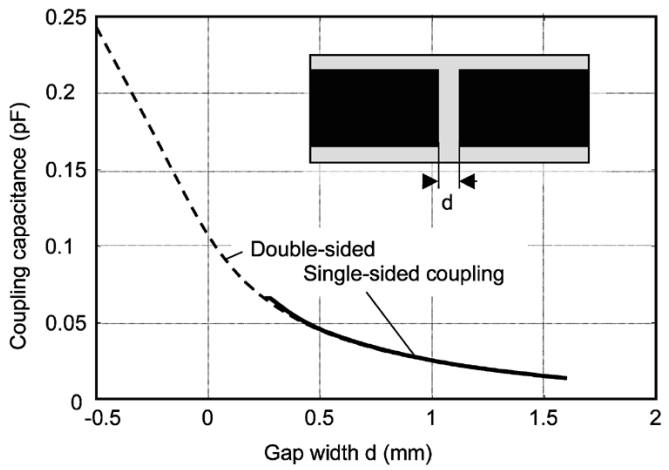

Fig. 4. Approximate capacitive values of end coupling (solid line: single layer coupling, dashed line: coupling between strips on opposite sides of the substrate). Negative gapwidth indicates overlapping of the strips.

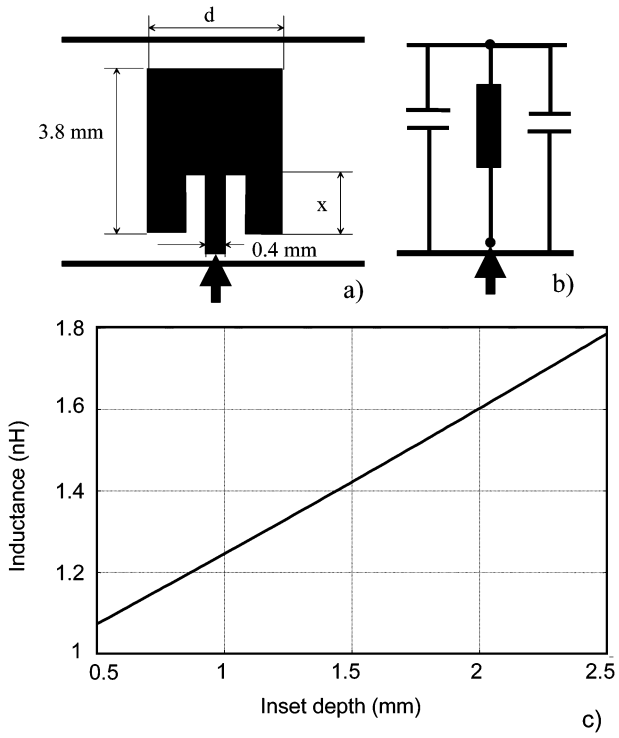

Fig. 5. (a) Layout of a shunt resonator. (b) Equivalent circuit of resonator (the ground connection of the inductance is opened to calculate the impedance at this interface). (c) Inductance versus inset depth. Patch width is $d = 2.6$ mm.

the thin strip to ground is plotted as a function of inset depths in Fig. 5(c). The capacitance of the patch is nearly independent of the inset depth of the inductive strip and can be adjusted by its width d.

In a similar way, all equivalent-circuit elements are obtained approximately by their respective SSL structure, and the overall geometry of the initial filter structure is determined.

This procedure is demonstrated at the example of a five-resonator bandpass filter, as shown in Fig. 6 (see [11] as well). To some extent, the filter layout resembles an interdigital filter with heavily loaded stubs; its design, however, is based on a classical lumped-element circuit. Center frequency, bandwidth, and

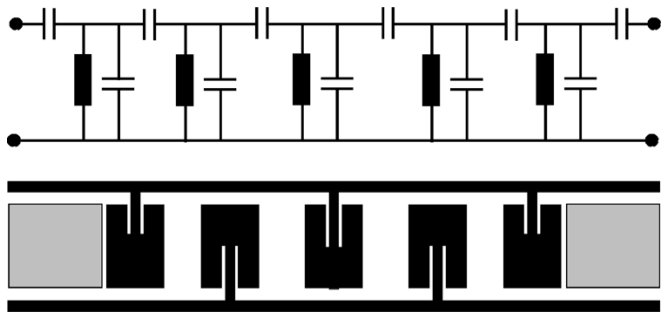

Fig. 6. Equivalent circuit and SSL layout of a five-resonator bandpass filter. (Grey elements: feeding lines on bottom side of the substrate.)

TABLE I
EQUIVALENT ELEMENT VALUES OF THE FILTER ACCORDING TO FIG. 6 (TOP)

C_{01} (pF)	0.096	C_1 (pF)	0.241	L_1 (nH)	1.08
C_{02} (pF)	0.018	C_2 (pF)	0.241	L_2 (nH)	1.4
C_{03} (pF)	0.012	C_3 (pF)	0.241	L_3 (nH)	1.43

TABLE II
GEOMETRICAL DIMENSIONS OF THE FILTER ACCORDING TO FIG. 6 (BOTTOM). THE NUMBERS IN BRACKETS GIVE THE FINAL DIMENSIONS AFTER OPTIMIZATION

No.	Coupling gap (mm)	Inset depth (mm)
1	0.05 (0.05) (double sided)	0.6 (1.35)
2	1.4 (1.75) (single sided)	1.4 (1.95)
3	1.8 (2.175) (single sided)	1.55 (1.95)

ripple were chosen to 8.2 GHz, 0.55 GHz, and 0.1 dB, respectively. The equivalent circuit can be derived according to standard filter design methods [10], in this case, selecting a constant shunt capacitance value of 0.241 pF according to patch widths of 2.6 mm. The respective SSL element dimensions can then be read using the diagrams in Figs. 4 and 5. For this filter, the input lines and resonators are placed on opposite sides of the substrate. Equivalent element values and geometrical dimensions are listed in Tables I and II.

The resulting SSL filter circuit is simulated based on its geometry, but typically, the results are different from the desired performance, as the starting geometry represents only a rough approximation of the desired elements. With increasing frequency, the lumped-element approach is no longer a sufficient description of the real structures, and electric and magnetic coupling between the different physical elements have not been taken into account. For the example filter, the initial simulation results are shown in Fig. 7. As experiences with such filters show, coupling gaps and inset depths are determined too low, resulting in an increased bandwidth, a higher center frequency, and incorrect resonances, especially of the outer resonators.

Thus, an optimization process has to be applied. In general, the optimization routines of commercial software might be used; these, however, take a very long computation time and often lead to suboptimal results due to local minima of the involved cost function. Therefore, a manual optimization is performed based on more sophisticated criteria like the behavior of each return-loss pole, position of return-loss maxima in the passband, etc. The procedure may be separated into two or three

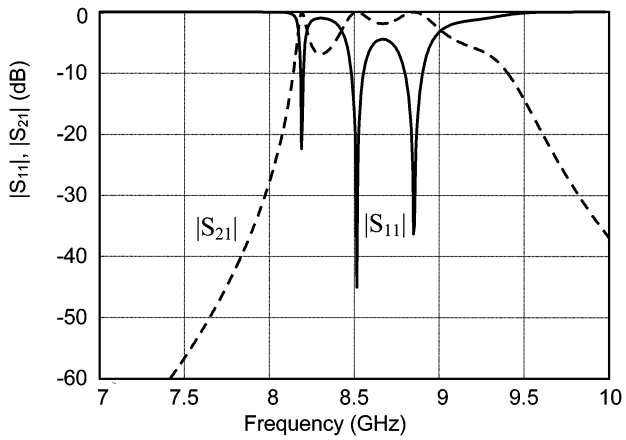

Fig. 7. Simulated results of the initial bandpass filter geometry.

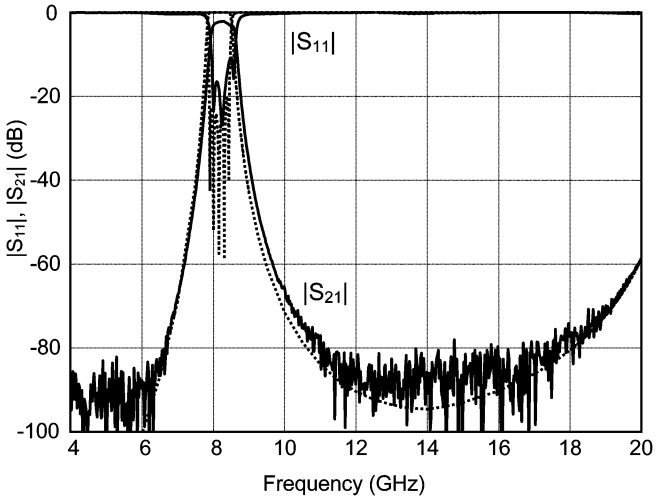

Fig. 8. Simulated and experimental results of a five-resonator bandpass filter. (Dotted lines: full-wave simulation. Solid lines: experiment.)

successive steps with different computational accuracy, leading to a considerable reduction of optimization time. Recently, a space-mapping approach was made using the lumped-element circuit for the coarse model and the geometrical structure for the fine model [12], together with a special optimizer applied to the coarse model to find global optima for the involved circuits.

The optimized geometry of the example filter is included in brackets in Table II; element dimensions had to be adjusted by a few tenths of a millimeter. Simulated and measured results of the filter finally are plotted in Fig. 8. Passband insertion loss is 2.1 dB. This increased loss is mainly due to the narrow inductive strips with deep insets. Simulations were done for single resonators assuming lossy metal; Q values of down to 150 were found for thin inductive strips and a deep inset, while this value increases up to 800 or 1000 for a wide strip and a short inset. For the same filter characteristics, however, the design procedure allows the selection of larger capacitances (larger patch width) and lower inductances with wider strips and shorter insets, thus insertion loss can be reduced significantly [11]. Due to the lumped-element character of the filter, a very wide stopband also results. Simulation and experiment agree well, except for an 80-MHz shift in center frequency due to the additional inductances provided by the groves in the mount.

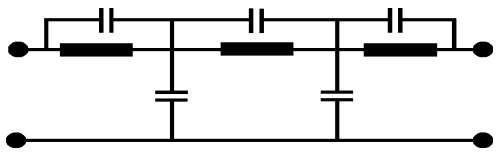

Fig. 9. Equivalent circuit of a low-pass filter with additional capacitive coupling parallel to the inductive elements.

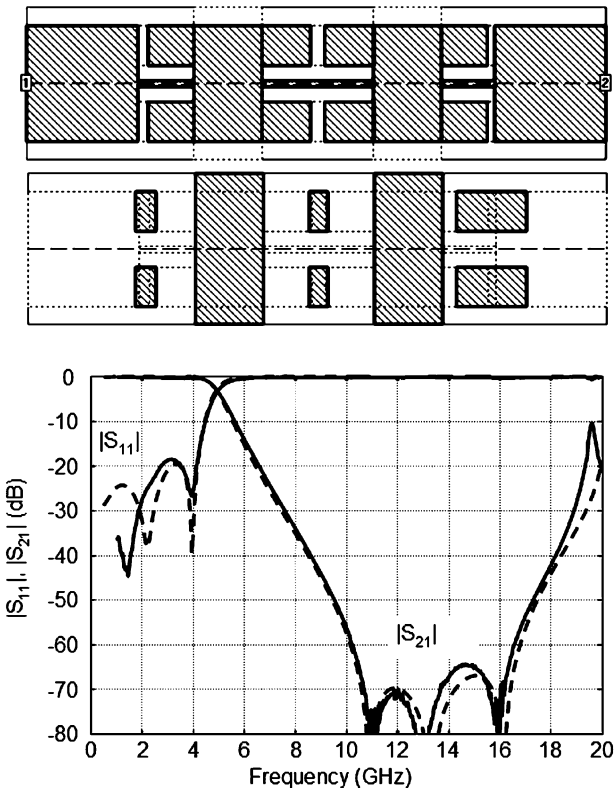

Fig. 10. Top and bottom layout and transmission performance of a low-pass filter with a threefold capacitive coupling. (Dashed lines: full-wave simulation. Solid lines: experiment.)

IV. Low-Pass Filter

The realization of low-pass filters consisting of short sections of very low impedance [see Fig. 2(a)] and very high impedance [see Fig. 3(a)] was demonstrated earlier [5]. As the inductive elements are very short, the metallization can be brought close together, and additional patches on the backside of the substrate can increase the respective capacitive coupling [see Fig. 3(d)]. This leads to additional coupling in parallel to the inductances (see [13, Figs. 9 and 10]). With a proper design of the elements, the resulting parallel resonators act like the required inductance at the corner frequency of the filter, but provide transmission zeroes at their resonance frequency. With different values for the respective elements in Fig. 9, three different transmission zeroes can be realized. Fig. 10 shows top and bottom metallization, as well as simulated and experimental results of such a filter with three transmission zeroes. The length of the filter itself amounts to approximately only 14 mm. Corner frequency is 4.2 GHz, and insertion loss is lower than 0.3 dB below 4 GHz including excess transmission-line length and the two transitions to the coaxial line. A stopband attenuation of better than 65 dB is achieved.

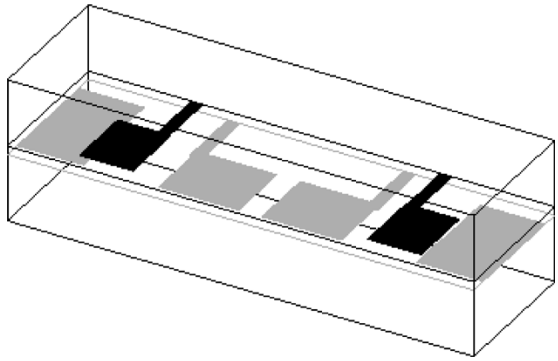

Fig. 11. Basic structure and layout of a four-resonator filter with transmission zeroes. (Black: top side of substrate. Grey: bottom side of the substrate.)

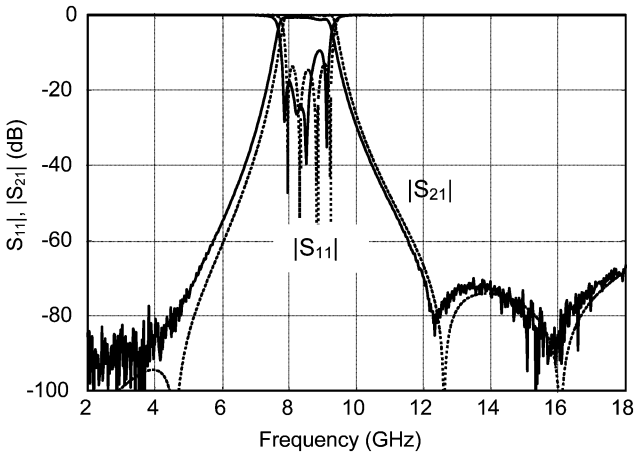

Fig. 12. Simulated and experimental return and insertion loss of the four-resonator filter. (Dotted lines: full-wave simulation. Solid lines: experiments.)

Theory and experiment show an excellent agreement down to −80 dB.

V. Bandpass Filters

A. Bandpass Filters With Coupled Parallel Resonators

A first bandpass filter with coupled resonators has already been demonstrated as a design example in Section III. If neighboring inductive strips are oriented to the same side, additional inductive coupling occurs, which can be modeled with a π equivalent circuit; this finally results in an inductance parallel to the respective coupling capacitor [14]. As with the low-pass filters, this can be exploited to generate additional transmission zeroes. Depending on the distance between the inductive strips, transmission zeroes can be realized both below and above the filter passband. The principle structure of a four-resonator filter with such additional magnetic coupling is shown in Fig. 11. Two resonators each are on opposite sides of the substrate, and due to multiple magnetic coupling, three transmission zeroes occur, as demonstrated in Fig. 12. Center frequency of the filter is 8.5 GHz, bandwidth amounts to 1.3 GHz, and passband insertion loss is 0.7 dB. The filter length (without connecting lines) is only 12 mm.

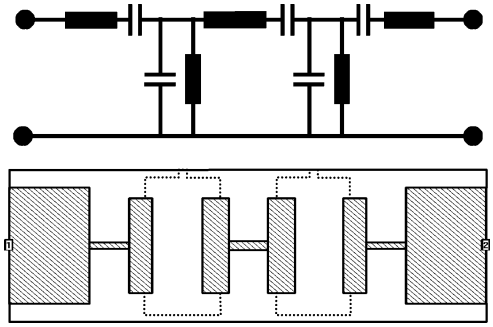

Fig. 13. Equivalent circuit and realization of a respective SSL bandpass filter with top (hatched) and bottom side (dotted) layout.

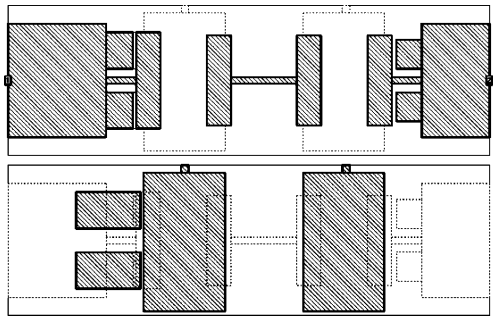

Fig. 14. Top and bottom side layouts of a five-resonator bandpass filter with additional transmission zeroes.

B. Bandpass Filters With Series and Parallel Resonators

Using the different elements, as introduced in Section II-B, even bandpass filters according to the classical ladder structure can be realized, consisting of series and parallel resonators [see Fig. 13 (top)]. A possible layout structure is shown in Fig. 13 below the equivalent circuit. The parallel resonators have the same SSL structure as those in the previous section, and the series resonators are composed of a narrow strip and a patch coupling to the parallel resonators. While the bandpass filters as shown before are most suited for narrow or medium bandwidth, the arrangements as presented here lend themselves to wide-band filters, as the element values for the series resonators would be too large for narrow bandwidth. According to the large bandwidth, filter slopes—at least at the upper band edge—get quite flat. To compensate for this, transmission zeroes may be generated by adding capacitive coupling in parallel to the inductors of the series resonators. This can be done easily by adding small metal sections to the connecting lines coupling to the capacitive patches, as shown in the layout of Fig. 14. Except for these elements, the remaining circuit is nearly unchanged. As a result, the filter performance, as given in Fig. 15, is achieved. The filter has a bandwidth of 6.8 GHz around 10 GHz. Filter length (without connecting lines) is 10.5 mm. Passband insertion loss amounts to 0.6 dB $\pm$0.1 dB. The peaks in insertion loss at 19 GHz are due to some mount resonance and higher order mode interaction.

VI. High-Pass Filter

If the resonator structures of a filter, as shown in Fig. 6 (bottom), are arranged alternatively on different substrate

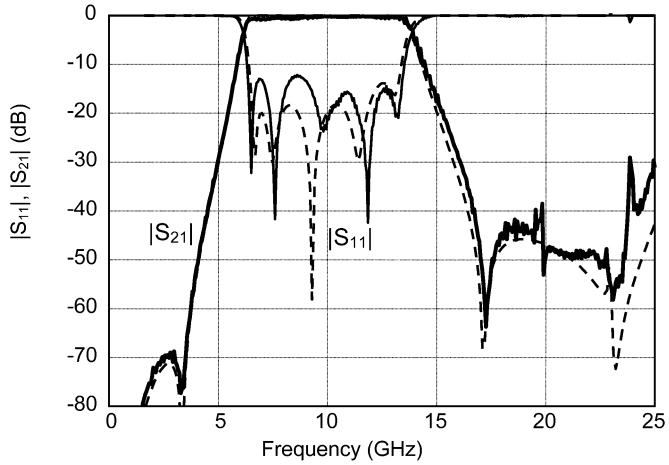

Fig. 15. Transmission characteristics of a five-resonator bandpass filter with additional transmission zeroes according to Fig. 14. (Dashed line: full-wave simulation. Solid line: experiment.)

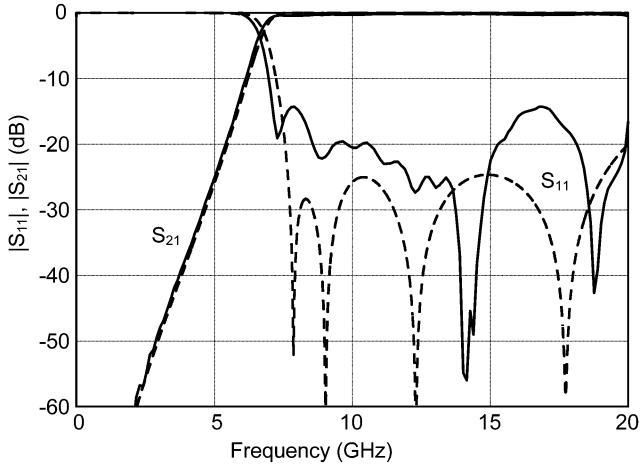

Fig. 17. Transmission characteristics of an SSL high-pass filter according to Fig. 16. (Dashed line: full-wave simulation. Solid line: experiment.)

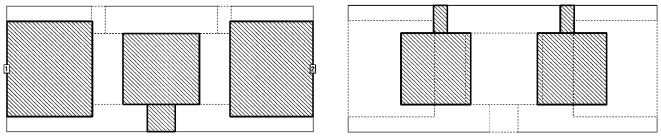

Fig. 16. Top (*left*) and bottom side (*right*) layouts of an SSL high-pass filter.

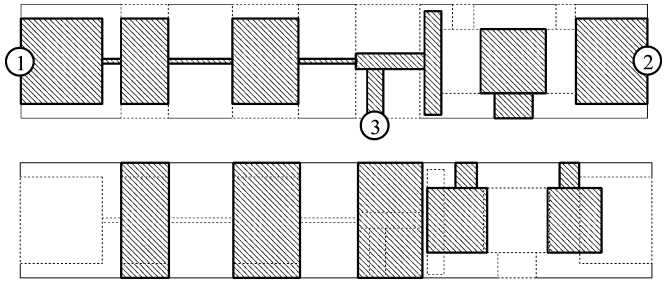

Fig. 18. Top and bottom side layouts of an SSL diplexer consisting of a low-pass (left-hand side) and a high-pass filter (right-hand side).

sides and brought together very close—the resonators typically overlap—high-pass filters result. Coupling between the resonator elements is made very strong in this way, and the capacitance of the patches against ground partly is shielded so that shunt inductances and series capacitances dominate. With proper design, high-pass filters with a very wide passband can be realized in this way. A typical layout of such a high-pass filter is given in Fig. 16. The corner frequency is 7.2 GHz, and high-pass performance with only a few tenths of a decibel of insertion loss is achieved up to more than 20 GHz (Fig. 17). The experimental return loss is somewhat higher than calculated; this is mostly due to an increasing return loss of the transitions to the coaxial measurement system.

VII. Diplexer

Based on the above reported results, the design of diplexers has also been investigated. In detail, the combination of low- and high-pass filters was considered (Fig. 18). With pure SSL filter structures, however, the T-junction to the common port is quite large due to the increased cross-sectional size of the SSL. This leads to a phase progression, which, at least for diplexers with broad-band filters, prevents good results. As a consequence, the involved T-junction was realized in the microstrip, and a SSL-to-microstrip transition was included into the design of the involved filters. For the low-pass filter, one of the outer inductive strips connects directly to microstrip. For the high-pass filter, one of the outer capacitive couplings is done by a patch connected to a microstrip line. To this end, the involved filters were redesigned. Only very short microstrip sections are involved so that the major advantage of low loss is maintained. The microstrip T-junction with linewidths of approximately 0.7 mm is quite small and includes only small phase shifts. The common port resulting in this way can easily be included in the commercial simulator maintaining a rectangular shielding box. In practice, however, the mount includes a T-shaped channel; thus, simulation and experimental setup do not completely match.

After joining the two filters via the T-junction, some redesign of the filter elements close to the junction was done to compensate for the effects of the T-junction and the influence of the respective other filter in order to get the desired diplexer results. In Fig. 18, the layout for both substrate sides of such a diplexer is shown, and a photograph of the diplexer is given in Fig. 19. The two transitions to microstrip and the microstrip T-junction can be seen clearly. Major simulated and experimental scattering parameters are plotted in Figs. 20 and 21. Low- and high-pass corner frequencies are 4.5 and 7.8 GHz, respectively. At 6.5 GHz, the two filters interact in such a way that there is a transmission zero of the low-pass filter insertion loss. The diplexer works fine up to 18 GHz, above this frequency, the return loss of the high-pass filter increases.

Some discrepancies between simulation and experiment, especially for the return loss at the high-pass side, are due to the differences in simulated and realized structure. While the simulation is based on a common port at the edge of the computation

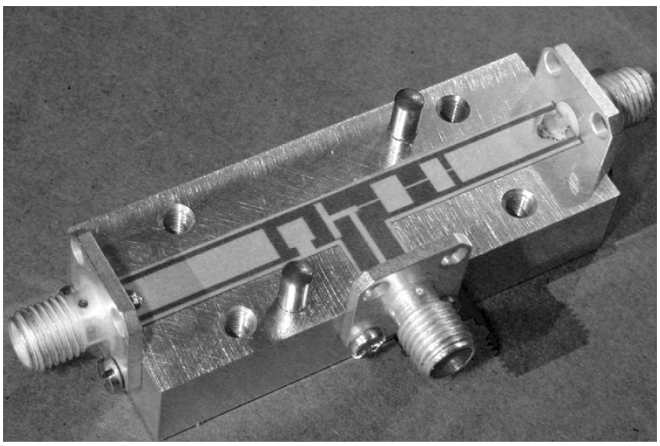

Fig. 19. SSL diplexer (compared to Fig. 18, left- and right-hand sides are interchanged as the layout mask was used face down).

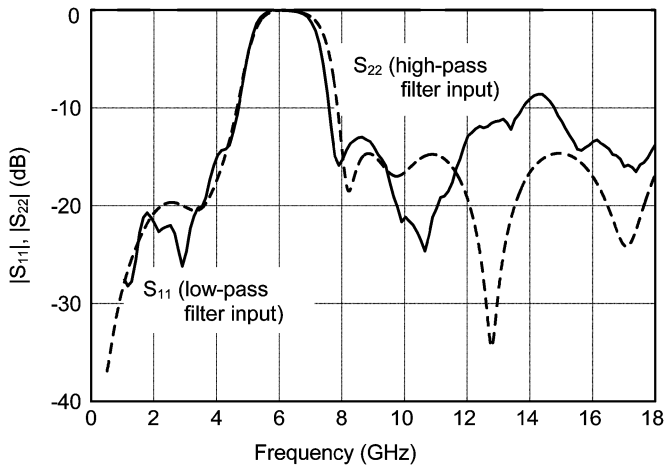

Fig. 20. Simulated and experimental return loss of the low- and high-pass input ports of the diplexer. (Dashed line: full-wave simulation. Solid line: experiment.)

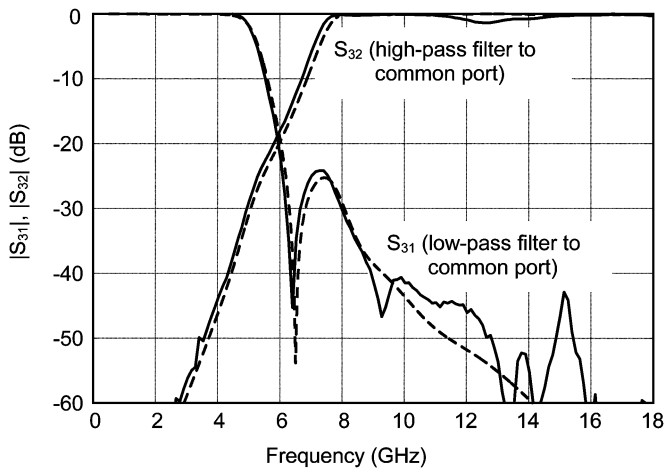

Fig. 21. Simulated and experimental insertion loss of low- and high-pass ports to the common port of the diplexer. (Dashed line: full-wave simulation. Solid line: experiment.)

box, a separate channel with the microstrip line is used for the hardware diplexer.

VIII. Conclusion

The SSL is well known as a low-loss medium for the realization of microwave filters. In this paper, a consequent extension to quasi-lumped element filters has been demonstrated. These elements provide capacitive coupling between strips on the same or the opposite side of the substrate, as well as toward ground, and both series and shunt inductive coupling by narrow lines. Even resonant couplings can be included, leading to transmission zeroes improving the stopband behavior of the filters. Basic reactance filter configurations are taken as starting point for the design, and full-wave calculation and optimization is used to account for the finite geometrical extension of the involved elements and for additional electromagnetic coupling, especially at higher frequencies. The simulation is done in a simple rectangular box, leading to acceptable computational efforts and excellent results compared to measurements. In the case of the diplexer, where the SSL cross section gets too large, an extension is made to include smaller microstrip structures to realize a small common port area.

References

[1] J. D. Rhodes, "Suspended substrates provide alternatives to coax," *Microwave Syst. News*, vol. 9, pp. 134–143, Aug. 1979.

[2] J. D. Rhodes and J. E. Dean, "MIC broad-band filters and contiguous diplexers," in *9th Eur. Microwave Conf. Dig.*, 1979, pp. 407–411.

[3] C. I. Mobbs and J. D. Rhodes, "A generalized Chebyshev suspended substrate stripline bandpass filter," *IEEE Trans. Microw. Theory Tech.*, vol. MTT-35, no. 5, pp. 397–402, May 1983.

[4] W. Schwab, F. Bögelsack, and W. Menzel, "Multilayer suspended stripline and coplanar line filters," *IEEE Trans. Microw. Theory Tech.*, vol. 46, no. 7, pp. 1403–1407, Jul. 1994.

[5] W. Menzel, "Broadband filter circuits using an extended suspended substrate transmission line configuration," in *22nd Eur. Microwave Conf.*, Helsinki, Finland, 1992, pp. 459–463.

[6] W. Menzel and F. Bögelsack, "Folded stubs for compact suspended stripline circuits," in *IEEE MTT-S Int. Microwave Symp. Dig.*, Atlanta, GA, Jun. 1993, pp. 593–596.

[7] E. Yamashita, M. Nakajima, and K. Atsuki, "Analysis method for generalized suspended striplines," *IEEE Trans. Microw. Theory Tech.*, vol. MTT-34, no. 12, pp. 1457–1463, Dec. 1986.

[8] E. Yamashita, B. Y. Wang, and K. Atsuki, "Effects of side-wall grooves on transmission characteristics of suspended strip lines," in *IEEE MTT-S Int. Microw. Symp. Dig.*, 1985, pp. 145–148.

[9] W. Schwab and W. Menzel, "On the design of planar microwave components using multilayer structures," *IEEE Trans. Microw. Theory Tech.*, vol. 40, no. 1, pp. 67–72, Jan. 1992.

[10] G. Matthaei, L. Young, and E. M. T. Jones, *Microwave Filters, Impedance Matching Networks, and Coupling Structures*. Norwood, MA: Artech House, 1980.

[11] W. Menzel, "A novel miniature suspended stripline filter," in *Eur. Microwave Conf.*, Munich, Germany, Oct. 2003, pp. 1047–1050.

[12] H. Bilzer, F. Frank, and W. Menzel, "A space mapping method allowing models with different parameter rank and physical meanings for coarse and fine model," in *IEEE MTT-S Int. Microwave Symp. Dig.*, Long Beach, CA, 2005. Session WEPD-1.

[13] W. Menzel and A. Balalem, "Compact suspended stripline quasi-elliptic low-pass filters," in *German Microwave Conf.*, Ulm, Germany, Apr. 2005, pp. 61–64.

[14] W. Menzel and M. Berry, "Quasi-lumped suspended stripline filters with adjustable transmission zeroes," in *IEEE MTT-S Int. Microwave Symp. Dig.*, Fort Worth, TX, 2004, pp. 1601–1604.

Wolfgang Menzel (M'89–SM'90–F'01) received the Dipl.-Ing. degree in electrical engineering from the Technical University of Aachen, Aachen, Germany, in 1974, and the Dr.-Ing. degree from the University of Duisburg, Duisburg, Germany, in 1977.

From 1979 to 1989, he was with the Millimeter-Wave Department, AEG, Ulm, Germany [now the European Aerospace, Defense, and Space Systems (EADS)]. From 1980 to 1985, he was Head of the Laboratory for Integrated Millimeter-Wave Circuits. From 1985 to 1989, he was Head of the entire Millimeter-Wave Department. During that time, his areas of interest included planar integrated circuits (mainly on the basis of fine-line techniques), planar antennas, and systems in the millimeter-wave frequency range. In 1989, he became a Full Professor with the Department of Microwave Techniques, University of Ulm, Ulm, Germany. His current areas of interest are multilayer planar circuits, waveguide filters and components, antennas, millimeter-wave and microwave interconnects and packaging, and millimeter-wave application and system aspects.

Dr. Menzel was an associate editor for the IEEE TRANSACTIONS ON MICROWAVE THEORY AND TECHNIQUES (2003–2005). From 1997 to 1999, he was a Distinguished Microwave Lecturer for Microwave/Millimeter Wave Packaging. From 1997 to 2001, he chaired the German IEEE Microwave Theory and Techniques (MTT)/Antennas and Propagation (AP) Chapter. He was the recipient of the 2002 European Microwave Prize.

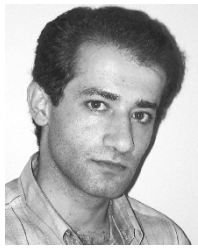

Atallah Balalem received the B.Sc. degree in physics (with a minor in electronics) from An-Najah National University, Nablus, Palestine, in 2000, and the M.Sc. degree in communications technology from University of Ulm, Ulm, Germany, in 2005. His Master's thesis concerned the design of very compact SSL filters and diplexers.

Since June 2005, he has been with Microwave and Communication Engineering, University of Magdeburg, Magdeburg, Germany.